polymer papers

# Magnetic orientation and microstructure of main-chain thermotropic copolyesters

**A. Anwer and A. H. Windle***
*Department of Materials Science and Metallurgy, University of Cambridge, Pembroke Street, Cambridge CB2 3QZ, UK*
*(Received 21 August 1992; revised 8 January 1993)*

The structural response of a molten main-chain liquid crystal polymer to an applied magnetic field has been investigated microscopically, with the microstructure being characterized as a function of field strength, time in the field and molecular weight. The application of the field to a structure in which the director wandered gradually on a scale of about 100 μm resulted in the formation of domains delineated by well defined boundaries. The domains were elongated along the field axis to an aspect ratio of about 8 in the case of a 1.1 T field, although for the higher field strength of 5.6 T the domains were no longer visible. Evidence is presented that the domain boundaries correspond to a director reorientation of π rad. Etched domain microstructure revealed a uniform distribution of crystallites, representing regions of local ordering in the material, on a scale of a few hundred nanometres. The crystallites had the form of platelets normal to the local director and acted as orientational markers across the domain boundaries.

**(Keywords: orientation; microstructure; copolyesters)**

## INTRODUCTION

The application of a magnetic field has a significant effect on the orientation of liquid crystalline materials through its interaction with the diamagnetic anisotropy of the molecules[1–9]. A single bond has its largest diamagnetic value for a field parallel to the bond axis and therefore tends to orient perpendicular to the field, although the reverse is true for double and triple bonds. The diamagnetic anisotropy is particularly marked in the case of aromatic ring molecules[10]. The susceptibility is much stronger for field directions normal to the plane of the ring than parallel to it. Where the rings are connected to form a polymer chain, the in-plane susceptibility will be greater along the chain axis than normal to it, especially where the links between the rings are highly conjugated. There will therefore be a tendency for polymer molecules to align with their chain axes parallel to a magnetic field. This effect will be especially apparent where the randomizing influence of thermal energy is reduced as a consequence of the molecules being orientationally ordered within a mesophase.

Magnetic orientation in nematic phases of various polymers has been studied since 1980 in several laboratories[11–18], and has been measured in both main-chain and side-chain materials by using X-ray diffraction[11,15], nuclear magnetic resonance (n.m.r.)[12,14] and measurements of the anisotropy of diamagnetic susceptibility[12,13]. However, the microstructural consequences have been less widely discussed and it is the aim of this paper to focus attention on this issue.

* To whom correspondence should be addressed

## EXPERIMENTAL

*Materials*

All the polymers studied were random copolymers of hydroxybenzoic and hydroxynaphthoic acids: in most

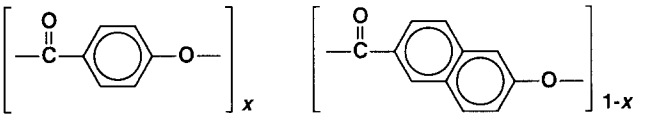

cases they were terminated by acid groups, with the molecular weight controlled by the addition of small amounts of terephthalic acid to the reactants. In the case of the material with the highest molecular weight there was no specific terminating group, and therefore the possibility existed that polymerization could continue during periods when the polymer was held in the melt.

The weight average molecular weights ($M_w$) (see *Table 1*) of samples **2–5** were measured by intrinsic viscosity, with the nominal $M_w$ of sample **1** equal to 6000, based on the not unreasonable assumption of a polydispersity for the condensation polymer of 2. Sample **6**, which is a commercial polymer (Vectra, from Hoechst Celanese Corporation), is often considered to have a *DP* of at least 150, and this is the value assumed here.

## RESULTS AND DISCUSSION

*Orientation kinetics*

The kinetics of orientation of this series of materials in a magnetic field has previously been reported by the authors[19]. *Figure 1* shows some recent orientational data for the polymer **1**, with a $M_w$ of 6000. These data were

0032-3861/93/163347-11

**Table 1** Weight average molecular weights ($M_w$) of the polymers used in these studies

| Sample | $M_w$ |
|---|---|
| **1** | 6000[a] |
| **2** | 4600[b] |
| **3** | 5000[b] |
| **4** | 8600[b] |
| **5** | 14 400[b] |
| **6** (Vectra[c]) | 36 000[d] |

[a] Nominal, on the basis of the amount of terephthalic acid added, and an assumed polydispersity of 2
[b] Measured by intrinsic viscosity
[c] Obtained from Hoechst Celanese Corporation
[d] Commonly accepted value for this material

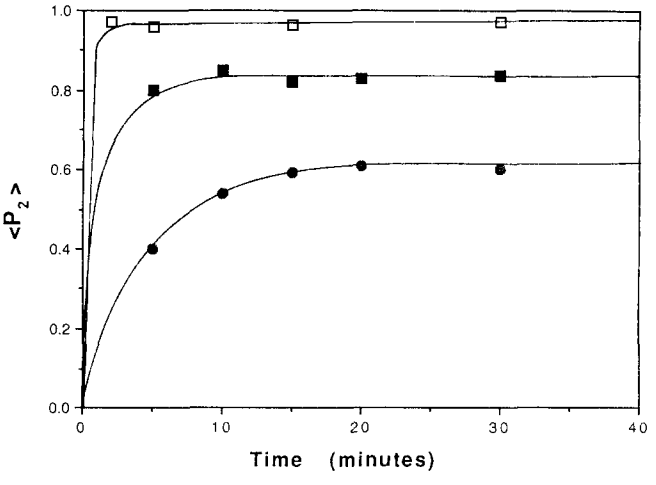


**Figure 1** Plots showing the development of the orientation with time at 300°C for polymer **1** ($M_w = 6000$) at different field strengths: (●) 0.55; (■) 1.1; and (□) 5.6 T

obtained from an analysis of the wide-angle X-ray diffraction patterns of samples that had been quenched after magnetic-field alignment in the melt. The analysis was based on the azimuthal distribution of the main equatorial diffraction maxima, with correction for the inherent width of the peak in the $z$-direction being made on the basis that, for a perfectly oriented sample, the peak would be equiaxial. The details of the method, as well as the basis for assuming that the crystallites exactly reproduce the parent melt orientation, have been discussed more fully in ref. 19.

The degree of preferred orientation, expressed as the second harmonic coefficient of the orientation distribution $\langle P_2 \rangle$, is plotted in *Figure 1* as a function of time in the field at 300°C for field strengths of 0.55, 1.1 and 5.6 T. The plateau values of orientation, i.e. $\langle P_2 \rangle_{max}$, were found to be 0.60, 0.85 and 0.97, respectively, for these three field strengths, while the corresponding characteristic time constants, $\tau$, were of the order of 25, 6, and 0.5 min, respectively.

The values obtained for $\langle P_2 \rangle_{max}$ and $\tau$ at the highest fields reported in ref. 19; in particular, the dependence of $\tau^{-1}$ on the square of the field strength is in accord with this new datum, as would be expected for any system where polarization is induced. The fact that the rate of orientation depends on the inverse square of the molecular weight emphasizes the need to use high fields if magnetic orientation is to be achieved in commercial polymers (with typical molecular weights) within a processing time frame that is realistic.

*Microstructure of polymer not subject to a field*

In all cases the polymer samples were prepared by melting a finely divided powder (~10 μm) which was obtained by milling the as-received material in a coffee grinder. The samples discussed in this section were held at a temperature of 30°C above the melting point (273°C in the case of $M_w = 600$) for 30 min in the absence of a field and then cooled at a rate of ~100°C min$^{-1}$.

*Figure 2* shows a micrograph of 20 μm thick section of a sample of polymer **1** in polarized light. This was prepared by wet grinding using, successively, 1200 and 4000 grit silicon carbide papers, and then finishing with 1 μm and then 0.25 μm diamond-impregnated medium-nap cloths. After the production of one polished flat, the specimen was mounted on to a glass slide using a very thin layer of epoxy resin, and the sample then ground down to the required thickness (within the range 20–40 μm). The intrusion of parallel scratches was minimized by coating the sample with microscope immersion oil, chosen with a refractive index between the two principal values for the oriented polymer. *Figure 2* shows no preferred orientation, with different local regions giving extinction at different settings of the crossed polars. The thin dark threads are disclinations characteristic of the nematic phase, the mean spacing of which is of the order of 100 μm. A further indication of the nature of the microstructure can be gathered from the examination of fracture surfaces. *Figure 3* shows the revealed microstructure for the same sample 'broken' at room temperature. It is apparent that the local orientation changes smoothly with position, i.e. gradually between the disclinations and more rapidly as the cores are approached. The mean traverse, before the director has rotated through 180°, is in the 100 μm range, which correlates with the optical micrograph. It is possible that the scale of the structure is in some way related to the particle size of the initial material, and further experiments are being planned to check for any such relationship. While it may seem to be reasonable to relate the fibril direction with the local director, further confirmation has been achieved by etching the fracture surface using 2% potassium permanganate in mixed sulfuric and phosphoric acids[20,21] to reveal the platelet crystallites, which are known to lie normal to the chain axes[22]. *Figure 4* shows an etched region centred on a disclination line. The very fine ridges, more apparent to the right of the micrograph, are the crystallites and at all times lie normal to the local axis of the fibrils.

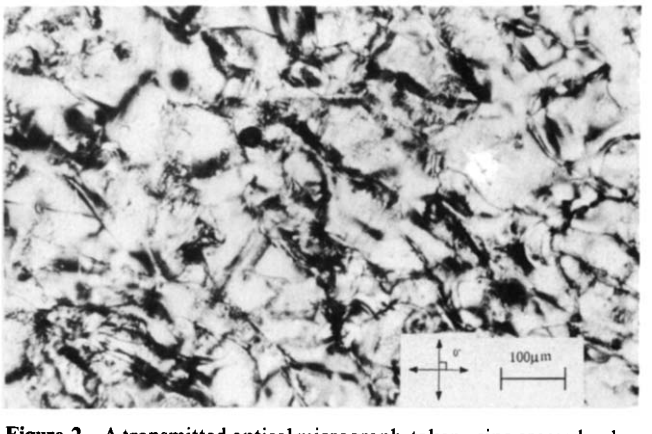


**Figure 2** A transmitted optical micrograph, taken using crossed polars (setting shown), of a 20 μm thick ground section of polymer **1** which had been held in the melt for 30 min, with no applied magnetic field

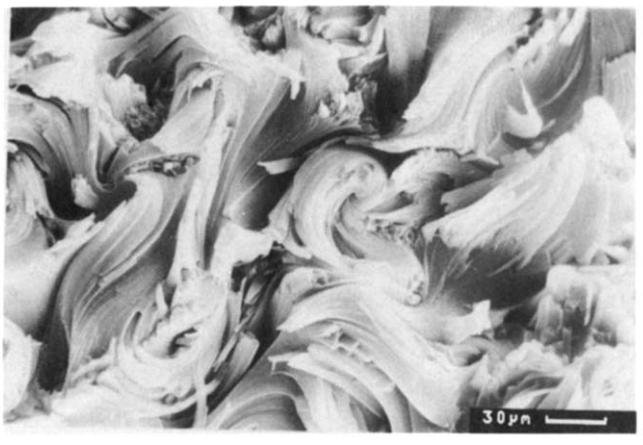


**Figure 3** A scanning electron micrograph of the fracture surface of the sample shown in *Figure 2*

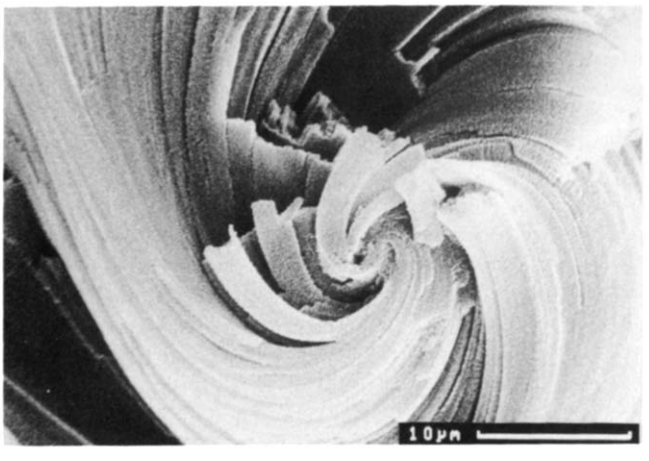


**Figure 4** Scanning electron micrograph showing details of the fracture surface in *Figure 3* after it had been etched to reveal crystallites which lie normal to the local chain axis

*Observations of the microstructures of polymer 1 oriented for 30 min in a field of 1.1 T at 300°C*

The application of a 1.1 T magnetic field leads to the development of domains within which the chains are oriented in the direction of the field. *Figure 5* shows a representative part of the microstructure as observed in a thin ground section between crossed polars. The thin horizontal lines are the result of the grinding operation. The optical orientation with the domains appears to be relatively uniform, but it changes rapidly across the boundary wall. *Figure 6* shows the variation in contrast on rotating the polars. When the polars are aligned with the field direction (*Figure 6d*) there is almost complete extinction within the domains. Such behaviour is consistent with the polymer within the domains aligning efficiently with the field, and all domains therefore showing a common orientation. Again it is clear that the boundaries represent a localized disruption in orientation. *Figures 7a* and *7b* show boundary details at a higher magnification. When the crossed polars are positioned for maximum transmission (see *Figure 7a*) the boundaries tend to appear as two dark lines against the white background, (e.g. C–D), whereas in the extinction geometry (see *Figure 7b*), all contrast is reversed and the appearance changes to a central dark line surrounded by two light bands against the dark background. The most straightforward interpretation of this behaviour is in terms of the boundary being essentially a bend distortion leading to a π-rotation of the chains, analogous to the so-called Néel walls in the parlance of ferromagnetic materials. The origins of the observed contrast are illustrated schematically in *Figure 8*. If the boundaries were to be of twist character, then a section normal to a boundary would view the molecules along the chain axes at the boundary centre, and thus the contrast would be expected to remain dark along the centre lines for all rotations of the polars. Such contrast was not often seen, even taking into account that not all boundaries would lie perpendicular to the section plane.

*Figure 9* represents an alternative method of revealing the domain boundaries. A sample is ground flat, and the surface is then etched prior to examination in the scanning electron microscope (SEM). The etching reveals the domain boundary network, with the vertical grooves being grinding artefacts. The domains are elongated in the direction of the field and it is apparent that the majority of the boundaries lie parallel to this. The method is more simple than the grinding of thin samples for transmission microscopy, as only one surface needs to be prepared and the problems of mounting a small sample in order to grind the second surface are avoided. It does, however, give rather less information about the structure and thickness of the domain boundaries, and the collective data discussed later in this paper were gathered using both of the techniques, as appropriate.

We thus conclude that the boundaries between the domains are largely of the bend type, presumably with some associated splay. The rotations across the boundary are π rad, with the polymer within the domains sharing a common orientation.

*Figure 10* is a transmission polarized light micrograph of a section ground normal to the magnetic field axis. Grinding in this orientation was particularly difficult, and it was not possible to get the sample thin enough to observe a full extinction contrast between the crossed polars (the crystallites scatter light too strongly in all sections that are greater than 20 μm thick). Any attempt to obtain thinner samples led to the removal of further pieces of material, and this has begun to happen in the sample shown in *Figure 10*, as is apparent from the circular black regions. However the network of boundaries is still visible, possibly as a consequence of

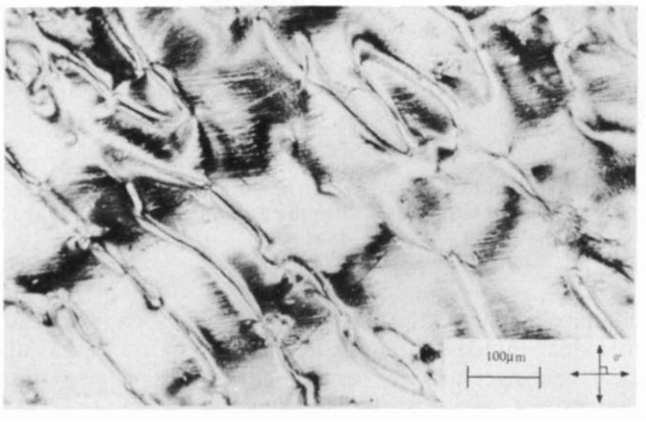


**Figure 5** A transmission optical micrograph, taken using crossed polars (setting shown) and sodium light, showing the domain structure in polymer **1** after the sample had been held at 300°C for 30 min in a field of 1.1 T. The magnetic field direction was diagonal from the top left to the bottom right; the fine horizontal lines were induced by the sample grinding process

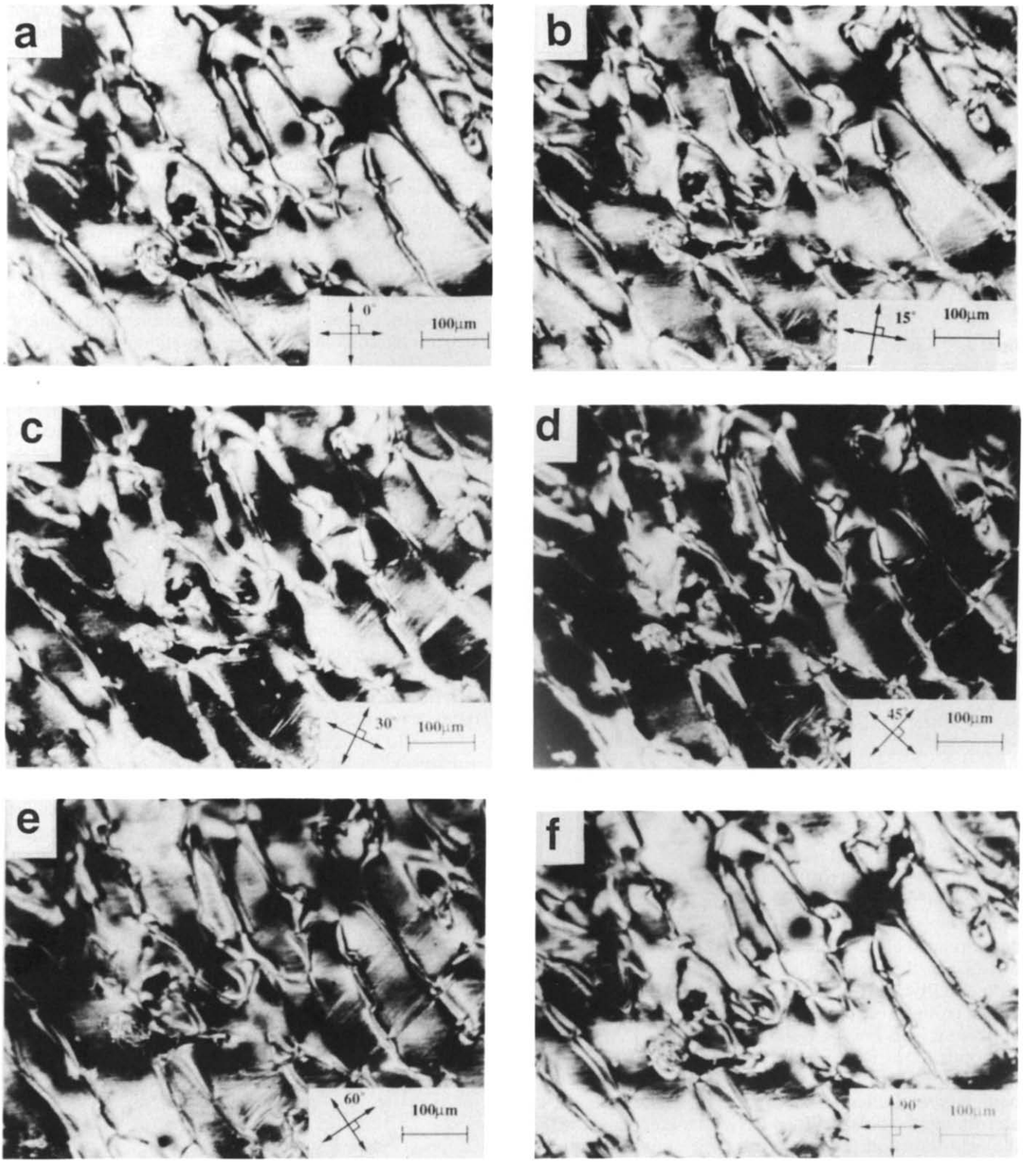


**Figure 6** A sequence of transmission optical micrographs of an area of a sample similar to that shown in *Figure 5*, prepared for different rotational settings of the crossed polars. When the polars are orthogonal to the field direction (from the top left to the bottom right) as in (d), there is almost complete extinction within the domains

enhanced light scattering in the boundary regions, and it is clear that the domains in this section are equiaxial, and their sizes are the same ($\sim 100\,\mu m$) as the smaller dimensions seen in the sections which contain the magnetic axis.

The preferred orientation induced by a 1.1 T field is very apparent in the fracture behaviour of the samples, which is fissile on planes parallel to the magnetic axis. Where fracture is induced across this axis the crack path frequently jumps planes, thus giving a 'stepped' appearance to the fracture surface. *Figure 11* shows such a fracture surface with the chains aligned vertically by the field. It is tempting to identify the regions of transverse fracture with the domains; certainly they are about the same size. However, the fracture surface does not provide any additional support for this view, especially as the alignment appears particularly good exactly in the areas where the crack is running parallel to the chain axis; this

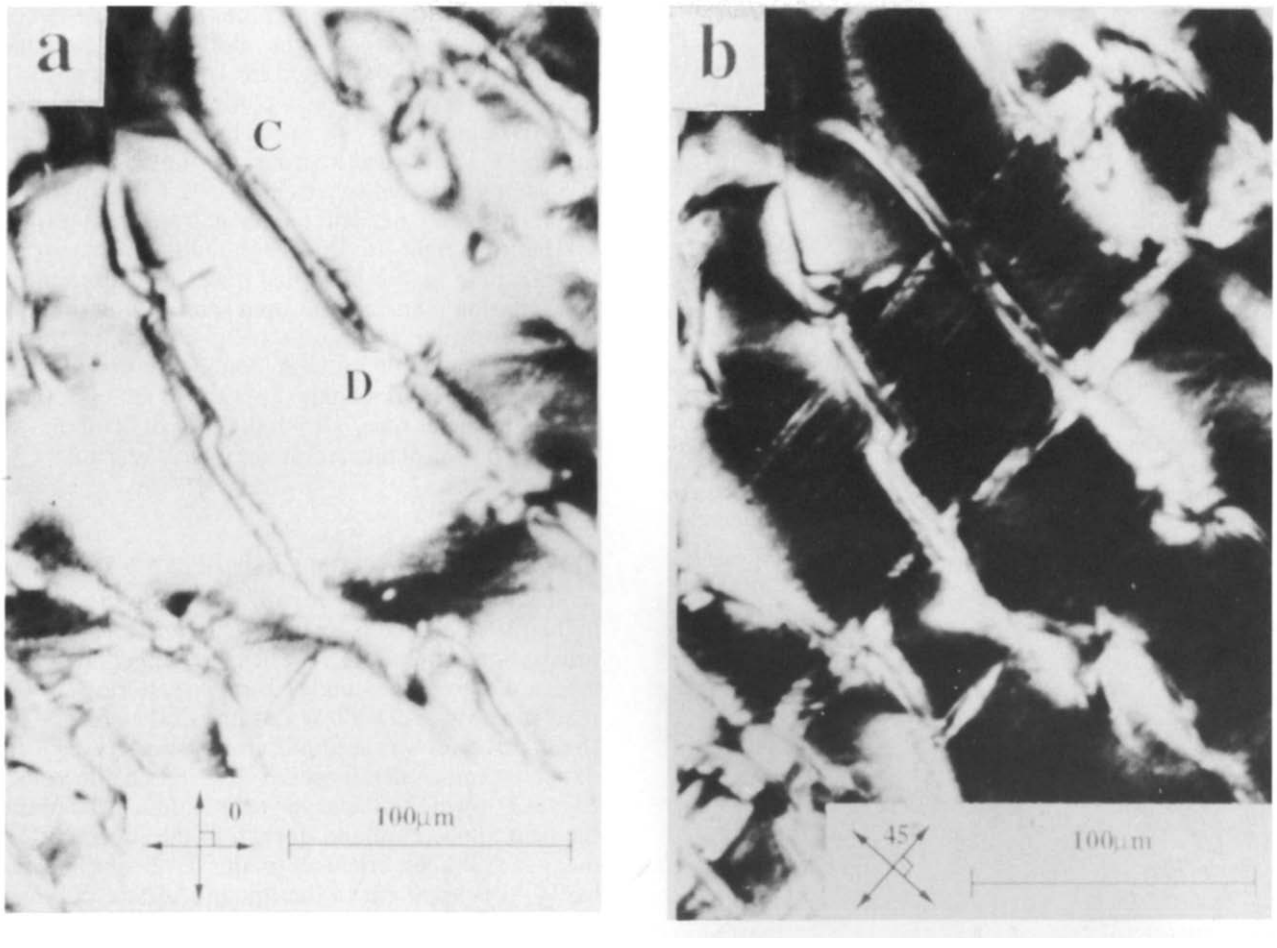


**Figure 7** The contrast associated with the domain boundaries in a section of polymer **1**, for two rotational settings of the crossed polars; the field alignment axis is from the top left to the bottom right of the figures

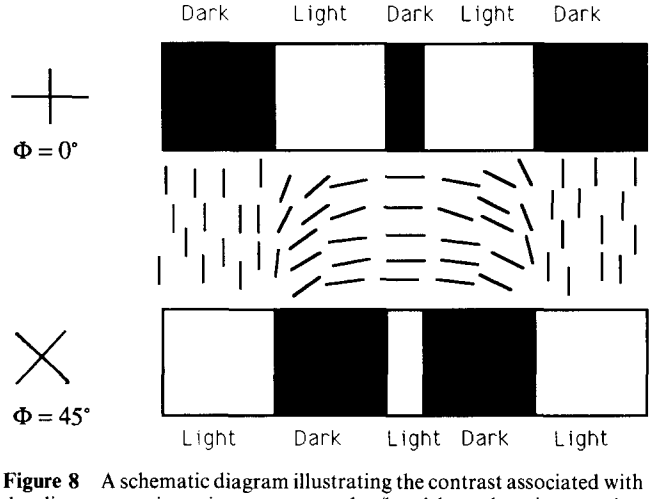


**Figure 8** A schematic diagram illustrating the contrast associated with the director reorientation across a splay/bend boundary in a section of polymer **1** for two settings of the crossed polars. The predicted contrast is in accord with that observed experimentally (see *Figure 7*)

would not be the case if the fracture path was along the domain boundaries. The radial texture seen on the transverse region is also intriguing, as it could conceivably indicate that the chain organization within the domains is not uniaxial. It is important to be cautious in this interpretation, however, as the radiating texture represents the local direction of crack propagation, the crack leaving its imprint on the surface as it jumps between the fissile layers that lie parallel to the field axis.

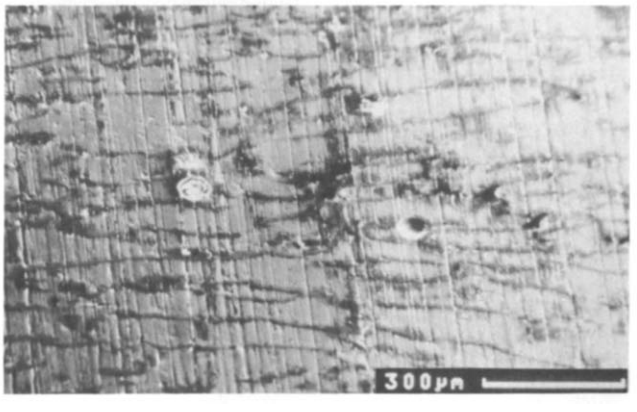


**Figure 9** The domain boundary network in a section of polymer **1**, as revealed by the surface grinding and etching technique, with the field applied in a horizontal direction across the page

*Observations of the microstructures of polymer I generated at 300°C in lower fields*

The microstructures described above illustrate 'before and after' states in that the application of a 1.1 T field for 30 min leads to a well developed domain structure. In order to follow the mechanism for domain formation a number of samples were examined after shorter exposures to lower fields. *Figure 12* is a fractograph of a sample oriented in a field of 0.55 T, for only 5 min. The field direction is from the top left to the bottom right on the photograph and the $\langle P_2 \rangle$ for this sample, measured by X-ray diffraction, is 0.4, i.e. about half the value

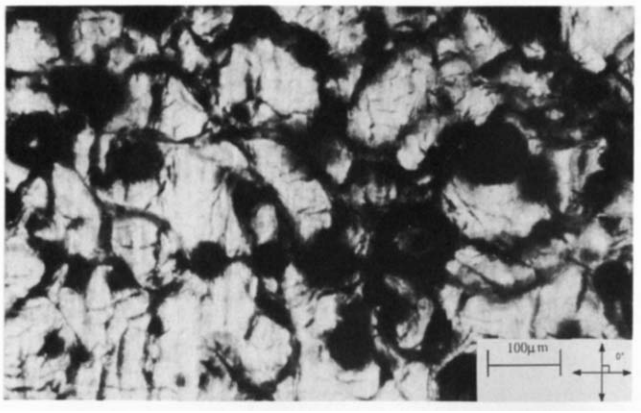


**Figure 10** A section of the same sample of polymer **1** as shown in *Figure 9*, but in this case ground normal to the magnetic orientation axis. The domains appear dark for all settings of the polars, but with an appropriate exposure the domain boundaries appear as a yet darker network. The dark discs correspond to areas of the thin sections that have been lost during the difficult grinding operation

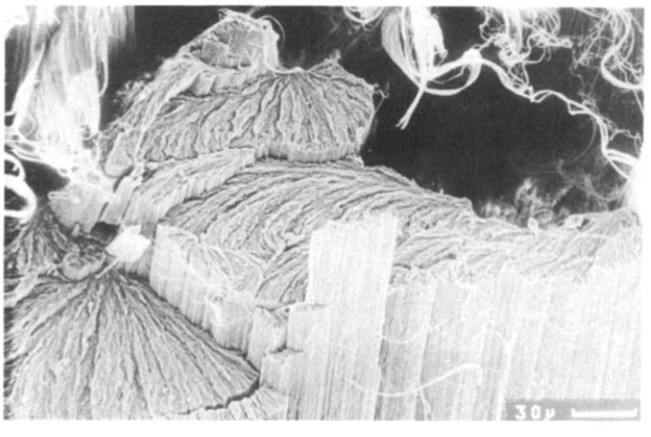


**Figure 11** An oblique SEM view of a fracture surface of an aligned sample of polymer **1**. The vertical striated surface (front right-hand side) is parallel to the vertical magnetic alignment axis, whereas the radial textured surfaces result from crack propagation that occurs normal to this axis

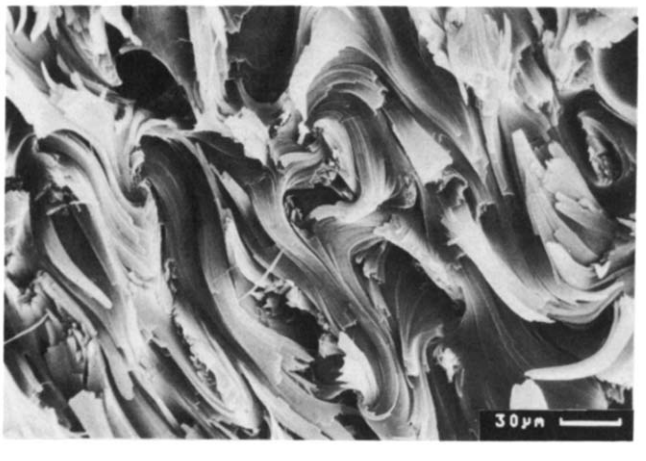


**Figure 12** The fracture surface of a sample of polymer **1** which had been weakly aligned in a field of 0.55 T for 5 min along the direction of the diagonal running from top left to bottom right. The $\langle P_2 \rangle$ of the sample was measured as 0.4

obtained for the higher-field sample, described above. The orientation appears to change continuously with position, as seen in the samples with no applied field, yet there is a distinct preferred orientation apparent in the field direction, with the curvature associated with the reversal in orientation showing signs of sharpening. It appears that with increasing times and/or field strengths the central regions of the domains in which the orientation is well developed in the direction of the field become increasingly extensive, while the poorly oriented areas become more and more localized as boundaries. *Figure 13* is an etched fractograph of a boundary region of a sample exposed to a field of 0.92 T for 5 min, which had a $\langle P_2 \rangle$ of 0.65. The field was from the bottom left to the top right in this case, and the curvature is sharper than in the previous, lower field example. The reorientation can be followed across the boundary, with the etched crystallites lying normal to the local director providing additional confidence in mapping the orientation. The boundary appears to be essentially of the splay–bend type, although it is difficult to assess whether out-of-plane components play any role.

*Microstructure of a sample oriented at 5.6 T*

The use of a superconducting magnet to produce much higher fields has led to samples with maximum preferred orientation which were very near to perfect, the $\langle P_2 \rangle$, as measured by wide-angle X-ray scattering (WAXS), reaching a value of 0.97. With times of the order of 1 min, the orientation was so rapid, in fact, that it was difficult to achieve much detail on the $\langle P_2 \rangle$ *versus* time plot (see *Figure 1*), owing to the experimental difficulties in timing the field application and quench in the superconducting magnet. Samples oriented to this level fibrillated very easily, as is apparent in the fracture surface of a sample of polymer **5** (which is parallel to the horizontal field direction) shown in *Figure 14*. However, the ease of fibrillation along the magnetic orientation axis, meant that it was impossible to grind the samples. Therefore, the only evidence which we have for domain boundaries comes from fracture surfaces such as those shown in *Figure 15* (note the etched crystallites). If one were to assume that this boundary was approximately normal to the fracture surface, then its general appearance would suggest a twist boundary, with the fibrils at its centre tending to lie normal to the surface. Boundaries of any sort were difficult to find on the fracture surface, and it was not possible to identify a network and thus assess a domain size. However, the observations were sufficient to enable a boundary width to be estimated.

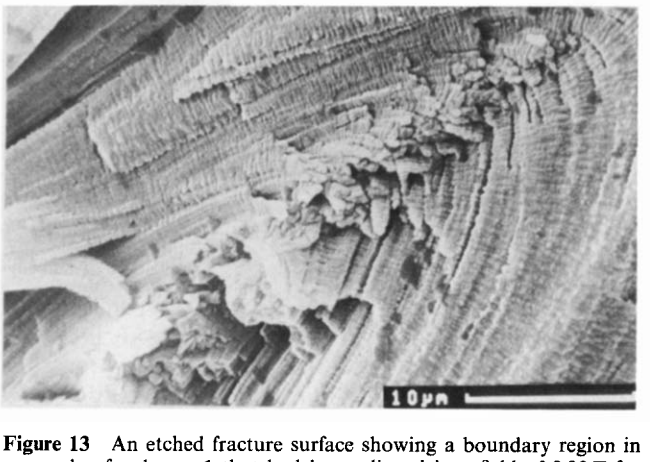


**Figure 13** An etched fracture surface showing a boundary region in a sample of polymer **1** that had been aligned in a field of 0.92 T for 5 min to give a $\langle P_2 \rangle$ of 0.65. The field axis in this case is from the bottom left to the top right of the figure

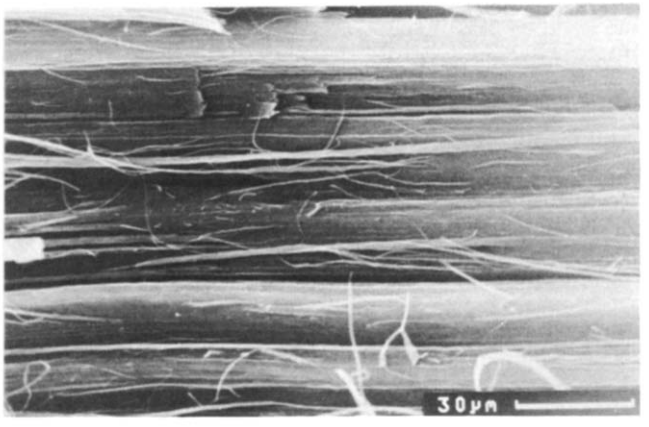


**Figure 14** A fracture surface containing the alignment axis (horizontal on the photograph) of a sample of polymer **5**, which has been oriented for 15 min in a field of 5.6 T at 320°C


**Figure 15** An etched fracture surface of the sample shown in *Figure 14*, showing a narrow boundary parallel to the horizontal field axis. The high quality of the alignment either side of the boundary, as indicated by the etched crystallites, is apparent

*Domain dimensions*

Three domain parameters, namely length, width and boundary width, have been measured as a function of the field strength using the microscopic techniques described above. The data obtained after the application of a field for 30 min at 300°C are summarized in the three plots of *Figure 16*. Measurements for the zero-field sample correspond to an estimate of the characteristic size of the microstructure and it should be emphasized that this microstructure does not consist of 'domains' as previously defined[23]. Despite the comparative sparseness of the data it is obvious that the domains get both longer and thinner with increasing field strength. The increase in length is approximately the same as the square of the decrease in width, which would suggest that the domain volume remains the same as the orientation develops. *Figure 16c* plots the domain volume, as (length) × (width)$^2$, and shows that the constant volume premise is not inconsistent with the data, bearing in mind the level of errors involved. It is intriguing to note that the increase in domain length by a factor of four on alignment is larger than would be expected from the field-induced rotations of the molecules, as the maximum axial extension which is achievable as the consequence of the perfect alignment of randomly oriented cylindrical molecules (of infinite axial ratio) is two[24]. The origins of the high level of domain extension that is observed are still being investigated, although it is important not to lose sight of the fact that there will be compensatory flow associated both with the different levels of orientation and thus extension within a domain, and also with the fact that the sample is contained within a boat and is thus unable to change its shape externally.

Ford *et al.*[25] reported that increasing the field strength decreased the lateral breadth of the boundary, an observation which was consistent with the theoretical predictions. *Figure 17* shows the data obtained for

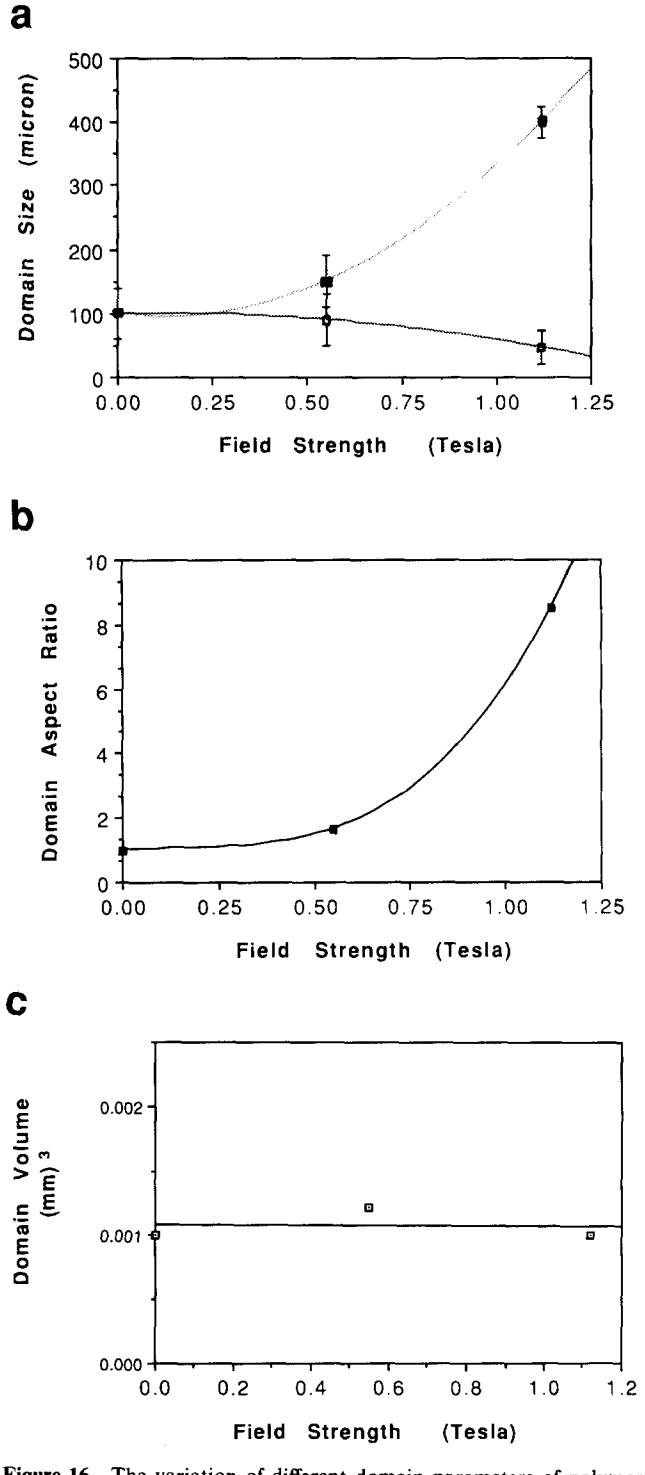


**Figure 16** The variation of different domain parameters of polymer **1** as a function of the field strength, with fields applied for 30 min at 300°C: (a) (■) mean domain length and (□) mean width; (b) domain aspect ratio; and (c) mean domain volume, calculated as (length) × (width)$^2$

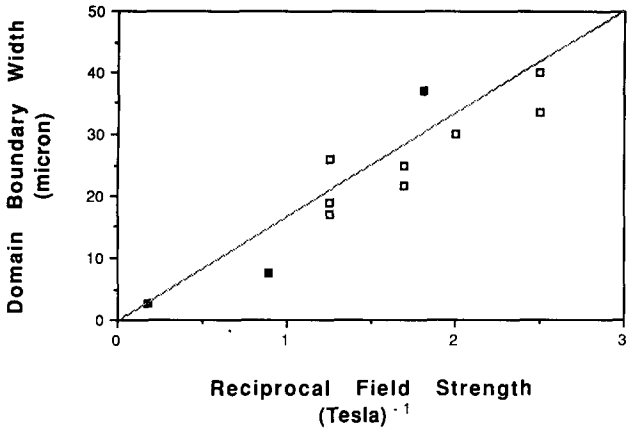


**Figure 17** The relationship between the domain boundary width of polymer **1** and the reciprocal of the applied field strength: (■) data obtained from the same series of experiments as in *Figure 16*, with the boundaries in general, parallel to the field axis, and (□) similar data (obtained from ref. 25) for a main-chain polyester with flexible sequences in the backbone

polymer **1**, from this series of experiments plotted as the boundary thickness against the reciprocal of the field strength. Also shown are the data from ref. 25, which refer to an aromatic polyester containing flexible sequences of seven ($CH_2$) units positioned periodically within the backbone. The slope of this plot is proportional to the square root of the elastic distortion energy and it is apparent that both types of main-chain polymer show similar behaviour. However, caution is necessary in deducing that the elastic constants are similar in each case, for it would be necessary first to assume that the anisotropy in the magnetic susceptibility is the same for each polymer; the further assumption that the splay, twist and bend components of the elastic distortion energy are equal is, itself, far from reasonable, especially in the case of polymeric mesophases in which the splay component is likely to be much larger than the other two[26]. The observation of the 'compression' of the boundaries by the field, but not, except possibly in the high-field situation (i.e. 5.6 T), of their elimination, provides a telling explanation of the measurements[19] that, for a given field, the orientation reaches a plateau value with time, and that the plateau level is higher for higher fields. A first-order check on this premise can be obtained by estimating the overall final orientation function $\langle P_2 \rangle_{max}$, on the basis that the polymer within the domains is perfectly aligned with the field axis while the orientation of that which forms the boundaries averages to zero. The volume fraction of material in the boundaries can be estimated from the sections examined, and in fact is equivalent to the ratio of boundary width to mean domain size as observed on a section. Because the boundaries measured were those parallel to the field axis, the domain size used is the lateral measurement. For perfect orientation, the coefficients $\langle P_0 \rangle$ and $\langle P_2 \rangle$ are both unity, while for the 'unoriented' boundary material, $\langle P_0 \rangle = 1$ and $\langle P_2 \rangle = 0$. Hence, $\langle P_2 \rangle_{max}$ for the sample as a whole can be given by: [(domain size)–(boundary width)]/(domain size). The values of $\langle P_2 \rangle_{max}$ estimated in this way are compared with the measured values for polymer **1** in *Table 2*. The agreement is surprisingly good, and further reinforces the view that the best orientation obtainable in a given field, i.e. $\langle P_2 \rangle_{max}$, is limited by the material comprising the domain boundaries. It is interesting to speculate on the situation for the high-field sample. Here $\langle P_2 \rangle_{max}$ has a value of 0.97 so that if the same trend was to continue, the domain width, for the measured boundary thickness of 2.8 μm, would now be about 85 μm. This result may be in keeping with the fact that we were not able to observe domains in the highly oriented samples, with the implication that the strong field is able to begin to eliminate boundaries, in addition to elongating the domains themselves.

*Involvement of surface fields*

The polymers studied provided opportunities for examining the combined influences of magnetic and surface fields on two counts. First, under certain conditions, bubbles form within the samples while they are held in the melt. In the case of the acid end-capped polymers, the bubbles began to show at melt treatments of 340°C and above, while at temperatures of 380°C or greater the internal gas that is generated begins to create a foam and all of the macroscopic preferred orientation is lost, irrespective of the field strength or duration[19]. *Figure 18* shows the fracture surface of polymer **6** after 30 min at 380°C; in cases such as these the source of the gas is thought to be the thermal degradation of the polymer. Isolated bubbles, which form at lower temperatures, serve as a good illustration of the disrupting influence of their surface on the general field-induced alignment. *Figure 19* shows a bubble which intersects a fracture surface of polymer **1**, which has been aligned along the horizontal axis of the photograph in a field of 1.1 T for 30 min. The tendency for the polymer molecules to lie parallel to the free surface of the bubble forces the local director pattern to 'flow' around it, thus disrupting the alignment with the magnetic field.

**Table 2** Comparison of the measured values of $\langle P_2 \rangle_{max}$ for polymer **1** (see *Figure 1*) with values estimated on the basis of microstructural observations

| $\langle P_2 \rangle_{max_1}$ [a] | Lateral domain size (μm) | Boundary width (μm) | $\langle P_2 \rangle_{max_2}$ [b] |
|---|---|---|---|
| 0.60 | 90 | 37 | 0.59 |
| 0.85 | 50 | 7.5 | 0.87 |

[a] Results obtained from WAXS measurements
[b] Estimated from microstructural observations

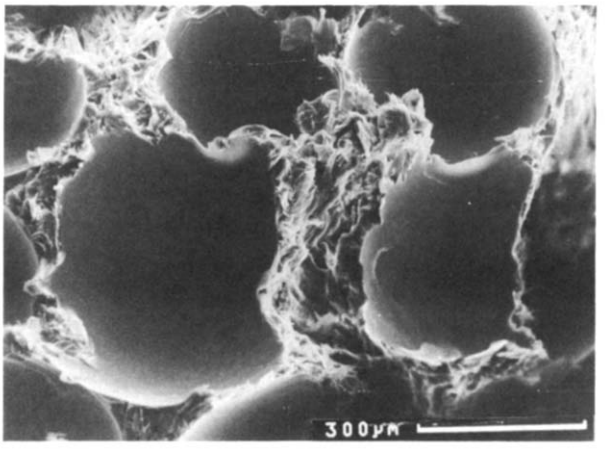


**Figure 18** The fracture surface of a sample of polymer **6** which had 'foamed' as a result of being held at 380°C for 30 min

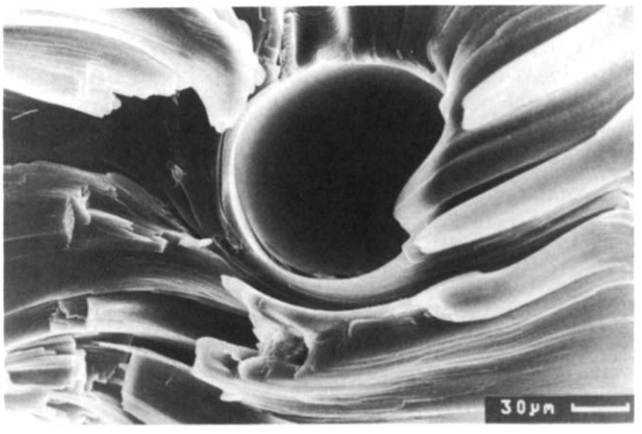


**Figure 19** An isolated bubble in a sample of polymer **1** which had been aligned in a field of 1.1 T for 30 min at 300°C. The field axis is horizontal, and the planar boundary conditions at the bubble surface have led to a local disruption in the orientation

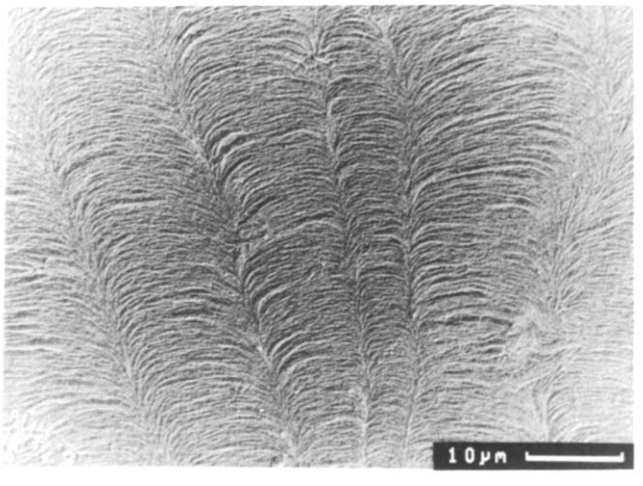


**Figure 20** The chain orientation on a free surface of polymer **5**, which has been revealed by etching of the crystallites which lie normal to the chain axes. This sample had been magnetically aligned in a 5.6 T field applied normal to its surface

Several unsuccessful attempts were made to orient high molecular weight benzoic–naphthoic (B–N) polymer **6** ($DP = 150$), for field strengths up to 5.6 T for 3 h. Kinetic measurements[19] indicate that, even at this molecular weight, significant alignment should be detectable after 30 min in even a 1.1 T field. The fact that it could not is thought to stem from the fact that the chain ends are still reactive and continuing polymerization in the melt not only takes the molecular weight and thus the viscosity to much higher levels, but also produces condensation products which contribute to the population of small bubbles, which then add their disruptive influence to any induced alignment.

A second type of interaction with a surface field was observed on the free surfaces of polymer **5**, which had been oriented in a field of 5.6 T for 15 min. The surface in this case is normal to the field axis, and the opposition of the vertical magnetic alignment in the bulk and the 'horizontal' planar alignment at the surface leads to the formation of a splay-compensated herringbone structure on the surface[27], which is revealed by means of crystallite etching (see *Figure 20*).

*Crystalline order*

While the etching of crystallites, especially on fracture surfaces, has been exploited in this work as a means of identifying the direction of the local chain axis, it is perhaps appropriate to consider the crystallite morphology in its own right, albeit briefly. The morphology in magnetically aligned samples is remarkable for its regularity, as can be seen in *Figure 21*. In particular, the length and straightness of the crystallites in their own planes (i.e. normal to the axes of the oriented chains) is greater than has been observed previously in any other type of sample, including drawn fibres[28]. The reasons for this remarkable level of organization are not yet clear. One possibility is that the chain segment segregation, which is a necessary precursor to the formation of crystallites from aperiodic random copolymer chains[22,29], is able to occur in the melt in the presence of a field. While there are other pointers to such behaviour[30,31], further studies will be necessary to properly understand the influence of fields on the crystallization process itself. The periodicity of crystallite spacing, i.e. the long period, was of the order of 70 nm, which is twice the value normally reported for these materials in fibre or sheared-film preparations[28], although similar values have been obtained after solid-state annealing[32]. The data presented in *Figure 22*, also underline the fact that there is no convincing evidence that the long period increases with the molecular weight.

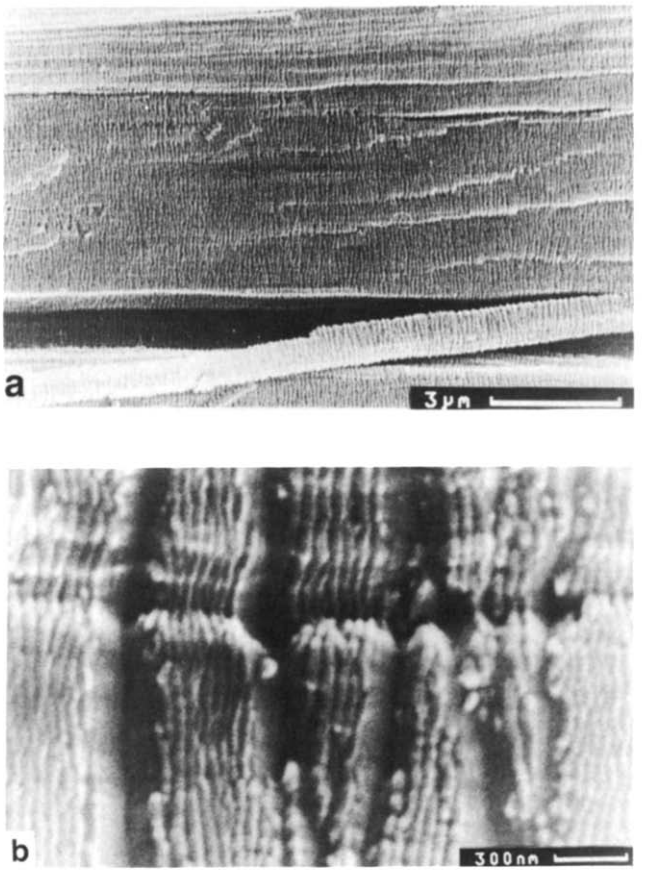


**Figure 21** Scanning electron micrographs of: (a), the etched fracture surface of polymer **5** aligned in a 5.6 T field, the axis of which is horizontal on the photograph, and (b), the same sample, shown at a higher magnification

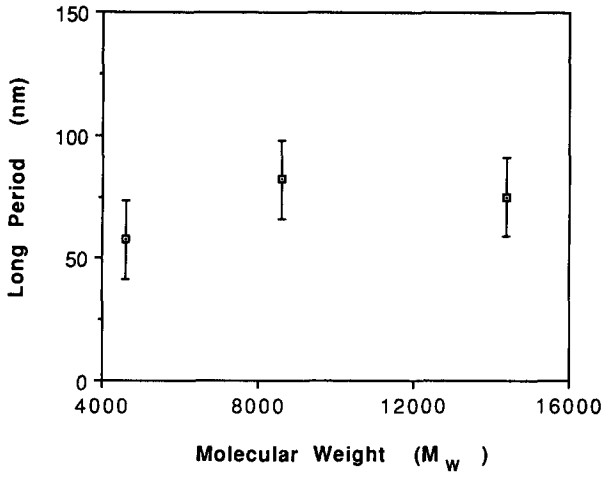


**Figure 22** Variation in the long periods of etched crystallites of samples of different polymers, as a function of their molecular weight

## CONCLUSIONS

1. The orientation kinetics shown by sample **1** ($M_w = 6000$) are in accord with those reported previously[19] for the series of copolymers, **2–5**. Orientation in the stronger field of 5.6 T was exceedingly rapid, as would be expected from the dependence of rate on the square of the applied field.
2. The microstructure of the polymer samples produced by melting a ground powder at 300°C, was shown to consist of smoothly wandering director fields in three dimensions, with the scale of the structure of the order of 100 $\mu$m. Surface fractography, and etch fractography which revealed crystallites as useful indicators of local director trajectory, showed the intersection of singularities with the surface. The structure seen in polarized-light microscopy was on a similar scale and revealed disclinations as the dark threads typical of the nematic.
3. The application of a field of 1.12 T for 30 min transformed the microstructure into domains within which the polymer was very well oriented. Overall, the orientation, $\langle P_2 \rangle_{max}$, was equal to 0.85. The domains were elongated in the direction of the field with an aspect ratio of the order of 8. Polarized microscopy of ground specimens indicated that most of the boundaries were of a splay–bend character and involved a director rotation of $\pi$ rad, observations which were in accord with the appearance of the boundaries on fracture surfaces. A section normal to the field axis showed an equiaxial boundary network.
4. At lower field strengths, the domains were less elongated and the boundaries were wider. On the other hand, the sample oriented in the 5.6 T field was very highly oriented ($\langle P_2 \rangle_{max} = 0.97$), but it did not show any clear boundary network. However, the boundaries that were seen were correspondingly narrower.
5. For fields increasing up to 1.1 T, the volume of the elongating domains appears to remain constant. It is, however, difficult to account for the observed level of domain extension in terms of molecular reorientation, alone.
6. The boundary width showed a reciprocal relationship with the field strength, in accord with earlier observations on a main-chain polymer containing flexible spacers[25].
7. The maximum 'equilibrium' orientation achieved at any field strength, $\langle P_2 \rangle_{max}$, can be accounted for on the basis of the simple assumption that the material within the domains is perfectly oriented, while that in the boundaries has no net orientation. The observed increase in $\langle P_2 \rangle_{max}$ with increasing field can thus be associated with a 'squeezing' of the boundaries by the field, and in the high field case (i.e. 5.6 T), with their partial elimination.
8. The tendency of the polymers in this series to assume a planar orientation at a free surface was seen to modify the director arrangement in the vicinity of bubbles, or (in the case of the 5.6 T specimens) close to a free surface which is normal to the field axis. The presence of bubbles, possibly as a consequence of degradation reactions or, in the case of polymer **6**, resulting from condensation products from a continuation of polymerization in the melt, disrupts the overall orientation and is probably the reason for the difficulty in obtaining magnetic orientation in polymers in which the molecules are not end-capped.
9. The crystallite morphology which is used here, after etching, as an additional indicator of local director orientation in the magnetically oriented samples, is also intriguing in its own right in that it appears much more regular than has previously been observed in shear-oriented polymer samples. Although not the major theme of this paper, observations in the magnetically oriented material of particularly well formed lamellae, and the occurrence of larger long-periods, which are not dependent on molecular weight, are nevertheless recorded.

## ACKNOWLEDGEMENTS

The authors are indebted to Hoechst Celanese Corporation of Summit, New Jersey, USA, for supplying the polymers and providing the relevant molecular weight information.

## REFERENCES

1 Krigbaum, W. R. in 'Polymer Liquid Crystals' (Eds A. Ciferri, W. R. Krigbaum and R. B. Meyer), Academic Press, London, 1982, Ch. 10
2 Talroze, R. U., Shibayev, V. P. and Plate, N. A. *Polym. Sci. USSR (Engl. Transl.)* 1983, **25**, 2863
3 Stupp, S. I. *Chem. Eng. Prog.* 1987, **83**, 17
4 Maret, G. and Blumstein, A. *Mol. Cryst. Liq. Cryst.* 1982, **88**, 295
5 Hardouin, F., Achard, M. F., Gasparoux, H., Liebert, L. and Strzelecki, L. *J. Polym. Sci., Polym. Phys. Edn* 1982, **20**, 975
6 Herlach, F. 'Strong and Ultrastrong Magnetic Fields and their Applications', Topics in Applied Physics Series, Vol. 57, Springer, Berlin, 1985
7 Moore R. C. and Denn, M. M. in 'High Modulus Polymers, Approaches to Design and Development' (Eds A. E. Zachariades and R. S. Porter), Marcel Dekker, New York, 1988, Ch. 6, p. 169
8 Moore, J. S. and Stupp, S. I. *J. Am. Chem. Soc.* 1987, **20**, 282
9 Moore, R. C. *PhD Thesis*, University of California at Berkeley, 1986
10 De Gennes, P. G. 'The Physics of Liquid Crystals', Clarendon Press, Oxford, 1974
11 Liebert, L., Strzelecki, L., van Luyen, D. and Levulut, A. M. *Eur. Polym. J.* 1981, **17**, 71
12 Maret, G., Blumstein, A. and Vilasagar, S. *Am. Chem. Soc. Div. Polym. Chem. Polym. Prepr.* 1981, **22**, 246
13 Noel, C., Monnerie, L., Achard, M. F., Hardouin, F., Sigaud, G. and Gasparoux, H. *Polymer* 1981, **22**, 578
14 Volino, F., Martins, A. F., Blumstein, R. B. and Blumstein, A. L. *J. Phys. Lett. (Paris)* 1981, **42**, 305
15 Maret, G. and Blumstein, A. *Mol. Cryst. Liq. Cryst.* 1982, **88**, 295

16 Hardouin, F., Achard, M. F., Gasparoux, H., Liebert, L. and Strzelecki, L. *J. Polym. Sci., Polym. Phys. Edn* 1982, **20**, 975
17 Sigaud, G., Yoon, D. Y. and Griffin, A. C. *Macromolecules* 1983, **16**, 875
18 Martins, A. F., Ferreira, J. B., Volino, F., Blumstein, A. and Blumstein, R. B. *Macromolecules* 1983, **16**, 279
19 Anwer, A. and Windle, A. H. *Polymer* 1991, **32**, 103
20 Olley, R. H. and Bassett, D. C. *Polymer* 1982, **23**, 1707
21 Windle, A. H., Dong, Y., Lemmon, T. J. and Spontak, R. J. in 'Frontiers of Macromolecular Science' (Eds T. Saegusa, T. Higashimura and A. Abe), Blackwell Scientific, Oxford, 1989, p. 343
22 Lemmon, T. J., Hanna, S. and Windle, A. H. *Polym. Commun.* 1989, **30**, 2
23 Windle, A. H., Viney, C., Golombok, R., Donald, A. M. and Mitchell, G. R. *Faraday Discuss. Chem. Soc.* 1985, **79**, 55
24 Brown, D. J. and Windle, A. H. *J. Mater. Sci.* 1984, **19**, 2013
25 Ford, J. R., Bassett, D. C., Ryan, T. G. and Mitchell, G. R. *Mol. Cryst. Liq. Cryst.* 1990, **180B**, 233
26 Meyer, R. B. in 'Polymer Liquid Crystals' (Eds A. Ciferri, W. R. Krigbaum and R. B. Meyer), Academic Press, London, 1982, Ch. 6
27 Kwiatkowski, M. and Hinrichsen, G. *J. Mater. Sci.* 1990, **25**, 1548
28 Hanna, S., Lemmon, T. J., Spontak, R. J. and Windle, A. H. *Polymer* 1992, **33**, 3
29 Hanna, S. and Windle, A. H. *Polymer* 1988, **29**, 207
30 Nicholson, T. M., Mackley, M. R. and Windle, A. H. *Polym. Commun.* 1992, **33**, 434
31 Golombok, R. *PhD Thesis* University of Cambridge, 1991
32 Wilson, D. J. and Windle, A. H. *Polymer* in press